



Universiteit  
Leiden  
The Netherlands

## **Novel interactions of Selenium Binding Protein family with the PICOT containing proteins AtGRXS14 and AtGRXS16 in Arabidopsis thaliana**

Valassakis, C.; Dervisi, I.; Agalou, A.; Papandreou, N.; Kapetsis, G.; Podia, V.; ... ; Roussis, A.

### **Citation**

Valassakis, C., Dervisi, I., Agalou, A., Papandreou, N., Kapetsis, G., Podia, V., ... Roussis, A. (2019). Novel interactions of Selenium Binding Protein family with the PICOT containing proteins AtGRXS14 and AtGRXS16 in Arabidopsis thaliana. *Plant Science*, 281, 102-112. doi:10.1016/j.plantsci.2019.01.021

Version: Publisher's Version

License: [Licensed under Article 25fa Copyright Act/Law \(Amendment Taverne\)](#)

Downloaded from: <https://hdl.handle.net/1887/3674350>

**Note:** To cite this publication please use the final published version (if applicable).



## Novel interactions of Selenium Binding Protein family with the PICOT containing proteins AtGRXS14 and AtGRXS16 in *Arabidopsis thaliana*

Chrysanthi Valassakis<sup>a,2</sup>, Irene Dervisi<sup>a,2</sup>, Adamantia Agalou<sup>c,1</sup>, Nikolaos Papandreou<sup>b</sup>, Georgios Kapetsis<sup>a</sup>, Varvara Podia<sup>a</sup>, Kosmas Haralampidis<sup>a</sup>, Vassiliki A. Iconomidou<sup>b</sup>, Herman P. Spink<sup>c</sup>, Andreas Roussis<sup>a,\*</sup>

<sup>a</sup> Department of Botany, Faculty of Biology, National & Kapodistrian University of Athens, 15784, Athens, Greece

<sup>b</sup> Department of Cell Biology and Biophysics, Faculty of Biology, National & Kapodistrian University, 15784, Athens, Greece

<sup>c</sup> Institute of Biology, Leiden University, Leiden, the Netherlands

### ARTICLE INFO

#### Keywords:

Selenium Binding Protein  
SBP1  
AtGRXS14  
AtGRXS16

### ABSTRACT

During abiotic stress the primary symptom of phytotoxicity can be ROS production which is strictly regulated by ROS scavenging pathways involving enzymatic and non-enzymatic antioxidants. Furthermore, ROS are well-described secondary messengers of cellular processes, while during the course of evolution, plants have accomplished high degree of control over ROS and used them as signalling molecules. Glutaredoxins (GRXs) are small and ubiquitous glutathione (GSH) -or thioredoxin reductase (TR)-dependent oxidoreductases belonging to the thioredoxin (TRX) superfamily which are conserved in most eukaryotes and prokaryotes. In *Arabidopsis thaliana* GRXs are subdivided into four classes playing a central role in oxidative stress responses and physiological functions. In this work, we describe a novel interaction of AtGRXS14 with the Selenium Binding Protein 1 (AtSBP1), a protein proposed to be integrated in a regulatory network that senses alterations in cellular redox state and acts towards its restoration. We further show that SBP protein family interacts with AtGRXS16 that also contains a PICOT domain, like AtGRXS14.

### 1. Introduction

Aerobic metabolism is characterised by the production of an unavoidable chemical entity that includes molecules collectively called reactive oxygen species (ROS) [1,2]. ROS, as by product of aerobic metabolism, include free radicals such as superoxide anion ( $O_2^{\cdot-}$ ), hydroxyl radical ( $\cdot OH$ ), as well as nonradical molecules like hydrogen peroxide ( $H_2O_2$ ), singlet oxygen ( $^1O_2$ ), and so forth. In plants, their production is strictly confined to cellular compartments with strong electron flow, and their formation is caused by the leakage of electrons to  $O_2$  from the electron transfer activities that chloroplasts, mitochondria and plasma membranes exhibit, or alternatively from metabolic pathways of different cellular compartments [3–5]. Their destructive activity is exerted by a wide range of physiological responses in plants, changes in cellular structure and the degradation of enzymes, proteins, nucleic acids, etc [2]. During abiotic stress the primary symptom of phytotoxicity can be ROS production which is strictly regulated by ROS scavenging pathways involving enzymatic and non-enzymatic

antioxidants. Furthermore, ROS are well-described secondary messengers of cellular processes including tolerance to environmental stresses [6–8], while during the course of evolution, plants have accomplished high degree of control over ROS and used them as signaling molecules [9]. Many studies have demonstrated the important role of ROS in signaling, such as the modulation of the activity of MAP kinases [10] and the stimulation of abiotic stress tolerance [11].

Glutaredoxins (GRXs) are small and ubiquitous glutathione (GSH) -or thioredoxin reductase (TR)-dependent oxidoreductases belonging to the thioredoxin (TRX) superfamily which are conserved in most eukaryotes and prokaryotes [12–15]. Roughly 30 different GRX isoforms have been identified in higher plants and in *Arabidopsis thaliana* GRXs are subdivided into four classes [16], playing a central role in oxidative stress responses and physiological functions [15,17,18]. In the last years, plant GRXs have been shown to participate in key developmental processes, as well [19–21]. Among the *Arabidopsis* class II GRXs, GRXS14 was recently shown to possess specific functions in the maintenance of chlorophyll content depending on environmental and light

\* Corresponding author.

E-mail address: [aroussis@biol.uoa.gr](mailto:aroussis@biol.uoa.gr) (A. Roussis).

<sup>1</sup> Current address: Developmental Biology, Biomedical Research Foundation Academy of Athens, Soranou Ephessiou 4, 11527, Athens, Greece.

<sup>2</sup> These authors contributed equally to this work.

**Table 1**  
Sequences of primers used in this study.

Primer name	Sequence
AtAy157988_F(Y2H)	CTCCCATATGGCTCTCCGATCTGTCAAACGCGG
AtAY157988_R(Y2H)	GAGGCTGCAGAGACACATAGCTTTCTCCACCTC
AtAY157989_F(Y2H)	CTCCCATATGGCTGCAATCACCATTCTTCCTCC
AtAY157989_R(H2Y)	GAGGCTGCAGGTTCAAGATATTGGCAAGTTCACC
HsSBP1-F-NdeI	CTCATATGGCTACGAAATGTGGG
HsSBP1-R-BamHI	TAGGGATCCAATCCAGATGTCAGAGCTAC
18S-F	TTGATTCTATGGGTGGTGGT
18S-R	CCTTGTACGACTTCTCCTT
RT-SBP1-F	CCGACTGGTCTCTTACCTTTG
RT-SBP1-R	CATCTTACTCCCTTTTTTATTCAACTC
RT-SBP2-F	TTGCATATTTATCAATGGCCT
RT-SBP2-R	GAGTAAGAACAACITTTAATTGTCT
RT-SBP3-F	GGCCCGGTTTACCAAAGGATTTG
RT-SBP3-R	CTGTTCCGATTTCCATAGAAATCCTTGATT
15803F	GATGAATTCATGGCGACGAAACGGAAGTTGTAGC
U15803Rsplit	CATCCCGGAATCCAGATATCGGAAGTGCAGTCTCC
15274F	GATGAATTCATGCAACCGAAACCGTATTAGCCACGGCCA
U15274Rsplit	CATCCCGGGATCCAGATATCGGAAGTGCAGTCTC
50289F	GATGAATTCATGGAAGCGGCGATGAACAACCCAGC
U50289Rsplit	CATCCCGGGAACCCAGATATCTGAGGTGCAGTCCGCCACC
T7-F	TAATACGACTCACTATAGGGGAATT
AtSBP1DEL1-R	GATATCCAGGTGGAGACTGC
AtSBP1DEL2-R	CTCGCTGTTTAGCGCATGG
AtSBP1DEL3-R	CAGTACAACATAGAGGACCC
AtSBP1DEL4-R	ACATGGAGCCATGAGGTTGT
AtSBP1DEL5-R	CAGCAGGTTGCTGATGGC
AtSBP1DEL6-R	GAGGGGAATGCTAAGGGG
AtSBP1DEL7-R	TGCCATGGTGATGCTTCTGT
AtSBP1DEL8-R	GCCGTCTACACCGGAAT
CXIP1F-NdeI	CATATGGCTCTCCGATCTGTCAA
CXIP1R-BamHIDE11	CATATGGCTCTCCGATCTGTCAA
CXIP1F-NdeIDE110	CATATGAAAGTGGTCTGTTTATGAAAGG
CXIP1R-BamHIDE11	GGATCCAGAGCACATAGCTTTCTCCAC
CXIP1-F-HindIII	AAGCTTCATGGCTCTCCGATCTGT
CXIP1-R-BamHI	GGATCCGAGAGCACATAGCTTTCTCC
CXIP2-F- EcoRI	GAATTCATGGCTGCAATCACATTTT
CXIP2-R-BamHI	GAATCCGGTTCAAGATATTGGCAAG

conditions [22].

AtGRXS14 (also referred to as AtCXIP1 or AtGRXcp) was initially isolated as a protein that associates with the cation exchanger of *Arabidopsis*, CAX1, a high capacity  $\text{Ca}^{2+}$  transporter [23]. AtGRXS14 contains a highly conserved through evolution PICOT domain and in a yeast expression system, it interacted with the N terminus of CAX1 in order to modify  $\text{H}^+/\text{Ca}^{2+}$  antiport activity [23]. Computational analysis revealed the similarity of AtGRXS14 to the yeast monothiol GRXs, the bacterial GRX4 and both zebrafish and mice GRX5 [24]. It has also been shown that loss of *AtGRXS14* (*AtGRXcp*) in *Arabidopsis* leads to protein oxidation in chloroplasts and seedlings sensitive to external oxidants, thus implicating a critical role of AtGRXS14 in redox state regulation in the chloroplasts [24].

It has been previously reported that AtGRXS14 (or AtCXIP1) interacts with AtSBP1 Selenium Binding Protein 1 (AtSBP1) [25]. Efforts to elucidate the biological role of SBP1 in plants have been made in the model legume *Lotus japonicus*, in *Arabidopsis thaliana* and rice [25–33]. Studies in *Arabidopsis* plants with altered endogenous levels of SBP1 suggested that there is a correlation between expression levels of the *Atsbp1* gene and tolerance to selenium toxicity caused by selenite [26]. Furthermore, it has been shown that SBP1 protein accumulates in response to cadmium (Cd) in *Arabidopsis* cultured cells [34] as well as in intact plants [27], while SBP1 overexpression confers enhanced tolerance to Cd thereby suggesting that this gene participates in a novel detoxification mechanism that plants use to overcome metal toxicity [27].

In this work, we characterize the novel interaction of AtGRXS14 with AtSBP1, a protein proposed to be integrated in a regulatory network that senses alterations in cellular redox state and acts towards its

restoration [35]. In vitro binding assays have shown that in *Arabidopsis* SBP1 participates in a novel protein network consisting of at least SBP, a NADP-dependent glyceraldehyde-3-phosphate dehydrogenase (GAPDH) and a fructose-bisphosphate aldolase (FBA), that is possibly part of the physiological regulation and metabolism of selenium [25] given the fact that in *Escherichia coli* GAPDH and a prokaryotic aldolase (deoxyribose-5-phosphate aldolase; DPA) were shown to bind selenium [36]. A major step towards understanding SBP1 function in plants and its involvement in Se metabolism and detoxification mechanisms was the identification of the selenium binding site and the involvement of two Cys residues in AtSBP1, as well as the function of selenite ( $\text{SeO}_3^{2-}$ ) reduction that this protein was shown to drive [33]. To further characterize the protein network that AtSBP1 protein participates in, we studied its interaction with AtGRXS14. Furthermore, we show that SBP protein family interacts with AtGRXS16 that also contains a PICOT domain, as AtGRXS14.

## 2. Material and methods

### 2.1. Yeast strains and plant materials

*S.cerevisiae* strain SG335 (MATa *trp1-901*, *leu2-3*, *112*, *ura1-52*, *his3-200*, *gal4Δ*, *gal80Δ*, *GAL2-ADE2*, *LYS2::GAL1-HIS3*, *met2::GAL7-lacZ*) was used in all yeast experiments in this study. Yeast two-hybrid screening was performed as described by Agalou et al. [25]. *Arabidopsis thaliana* ecotype Columbia (Col-0) and transgenic *Arabidopsis* plants harbouring SBPs::GFP and GRXs::GFP expression cassettes were used in the present study. Growth conditions were described in Valassakis et al. [35].

## 2.2. Nucleic acid extraction and cDNA synthesis

Total RNA was extracted from plant tissues using the procedure described by Onate-Sanchez and Vicente Carbajosa [37]. RNA samples were treated with DNase I (Biolabs, Ipswich, England) according to the manufacturer's instructions. The RNA purity and quantity were checked by electrophoresis in a 0.8% w/v agarose gel. Following electrophoresis, the RNA was stained with ethidium bromide (100 µg/l, Sigma Aldrich) and visualized under UV light. First-strand cDNA synthesis was performed using 1 µg of total RNA template and PrimeScript Reverse Transcriptase (Takara-Clontech, Kyoto, Japan). All PCR reactions were performed in a thermal cycler (Applied Biosystems, Foster City, CA, USA).

PCR products for cloning were amplified with Phusion High-Fidelity DNA Polymerase (New England Biolabs, Beverly, MA, USA) according to the manufacturer's instructions. In particular, for the isolation of *Arabidopsis thaliana* GRXS14 and GRXS16 cDNA was synthesized from total RNA of 10-days-old wild type *A. thaliana* (L.) Heynh (ecotype Columbia-0) seedlings and the following sets of primers were used: AtGRXS14: AtAy157988\_F(Y2H), AtAY15798\_R(Y2H), AtGRXS16: AtAY157989\_F(Y2H), AtAY157989\_R(H2Y) (Table 1). For the isolation of human SBP1 cDNA, total RNA from *Homo sapiens* (kindly provided by Prof. P. Kollia) was used and PCR was performed using HsSBP1-F-NdeI and HsSBP1-R-BamHI primers (Table 1). PCR products were separated by electrophoresis on 1% agarose gels, visualized under UV light after staining with ethidium bromide (100 µg/l, Sigma Aldrich) and purified using a Nucleospin Gel and PCR Clean up kit (Macherey-Nagel, Duren, Germany). Finally, the isolated cDNAs were cloned into the pJET1.2/blunt Cloning Vector (CloneJET™ PCR Cloning Kit, Thermo Scientific™) and sequenced.

## 2.3. Treatment of plants and gene expression analysis

*Arabidopsis* seeds plated on half-strength MS medium were grown vertically for 4 days. At this point, young seedlings were transplanted onto plates containing half-strength MS medium plus either of 150 µM sodium selenite (Na<sub>2</sub>SeO<sub>3</sub>, Sigma-Aldrich), 150 µM sodium selenate (Na<sub>2</sub>SeO<sub>4</sub>, Alfa Aesar, Karlsruhe, Germany) or 150 µM cadmium chloride (CdCl<sub>2</sub>, Sigma-Aldrich) and grown under the conditions mentioned above for 6 additional days. The chemicals used for the treatments were maintained as 50 mM stock solutions in distilled water. Seedlings transplanted onto plates containing only half-strength MS medium were used as controls. Roots from 10-days-old control and treated seedlings were collected, weighed, frozen in liquid nitrogen and stored at –80 °C for further use in semi-quantitative RT-PCR analysis.

cDNA was synthesized from total RNA extracted from plant tissues grown in physiological conditions (3-days-old and 10-days-old seedlings, roots, cotyledons and shoots/leaves from 10-days-old seedlings, rosette leaves and flowers from mature plants) and from 10-days-old roots treated as described above.

For semiquantitative RT-PCR, the Kapa Taq PCR Kit (Kapa Biosystems, Woburn, MA, USA) was used according to manufacturer's instructions. All PCR products were separated by electrophoresis on 1–1.2% agarose gels and visualized under UV light after staining with ethidium bromide (100 µg/l, SigmaAldrich). The primers used to amplify the genes of interest are listed below: 18S-F, 18S-R, SBP1: RT-SBP1-F, RT-SBP1-R, SBP2: RT-SBP2-F, RT-SBP2-R, SBP3: RT-SBP3-F, RT-SBP3-R, GRXS14: AtAy157988\_F(Y2H), AtAY157988\_R(Y2H), GRXS16: AtAY157989\_F(Y2H), AtAY157989\_R(H2Y) (Table 1). Densitometric analysis was performed with the GELEval (Frogdance) software.

## 2.4. Constructs for yeast assays

In the present study pGADT7 and pGBKT7 provided from Clontech were used as yeast vectors. ORFs from *AtSBPs*, *HsSBP1* and *AtGRXS*

were amplified from the respective pJET1.2 clones with specific pairs of primers using Phusion High-Fidelity DNA Polymerase (New England Biolabs, Beverly, MA, USA) according to the manufacturer's instructions. These primers introduced *NdeI* and *SmaI* ends at the 5' and 3' ends of the amplified sequences of *AtSBP1*, *AtSBP2* and *AtSBP3*, *NdeI* and *BamHI* sites in the *HsSBP* and *NdeI* and *PstI* sites in the *AtGRXS*. PCR products were purified using a Nucleospin Gel and PCR Clean up kit (Macherey-Nagel, Duren, Germany) and cloned into yeast vectors. Particularly, *AtSBP1*, *AtSBP2*, *AtSBP3* and *HsSBP1* were cloned into the pGADT7 vector while *GRXS14* and *GRXS16* into the pGBKT7 vector. Furthermore, eight fragments of the coding region of *AtSBP1* resulting from the sequential deletion of its nucleotide sequence (*AtSBP1DEL1-8*) were cloned into the pGADT7 vector with *NdeI/BamHI* sites, as well as two fragments of the *AtGRXS14* (*AtGRXS14* +/- PICOT) with *NdeI/BamHI* sites into the pGBKT7 vector. There was also swap of coding regions-vectors, where it was necessary. The sets of primers used are listed below: *AtSBP1*: 15,803F, U15803Rsplit, *AtSBP2*: 15,274F, U15274Rsplit, *AtSBP3*: 50,289F, U50289Rsplit, *HsSBP1*: *HsSBP1-F-NdeI*, *HsSBP1-R-BamHI*, *GRXS14*: AtAy157988\_F(Y2H), AtAY15798\_R(Y2H), *GRXS16*: AtAY157989\_F(Y2H), AtAY157989\_R(H2Y), *AtSBP1DEL1*: T7-F, *AtSBP1DEL1-R*, *AtSBP1DEL2*: T7-F, *AtSBP1DEL2-R*, *AtSBP1DEL3*: T7-F, *AtSBP1DEL3-R*, *AtSBP1DEL4*: T7-F, *AtSBP1DEL4-R*, *AtSBP1DEL5*: T7-F, *AtSBP1DEL5-R*, *AtSBP1DEL6*: T7-F, *AtSBP1DEL6-R*, *AtSBP1DEL7*: T7-F, *AtSBP1DEL7-R*, *AtSBP1DEL8*: T7-F, *AtSBP1DEL8-R*, *AtGRXS14* + PICOT: CXIP1F-NdeI, CXIP1R-BamHI, *AtGRXS14* –PICOT: CXIP1F-NdeI, CXIP1R-BamHI (Table 1).

## 2.5. Construction of vectors for plant transformation

Subcellular localization experiments of the *AtSBP* and *AtGRX* proteins were carried out by using pSAT6.eGFP-N1 vector [38]. In brief, the full-length coding regions of *AtSBPs* were extracted from the same pJET1.2 plasmids used in yeast transformation, described above, using *EcoRI/XmaI* as restriction enzymes, purified using a Nucleospin Gel and PCR Clean up kit (Macherey-Nagel, Duren, Germany), and cloned into pSAT6.eGFP-N1 vector, in frame with N-terminus of eGFP protein. The full length ORFs of *AtGRXS14* and *AtGRXS16* were PCR amplified using Phusion High-Fidelity DNA Polymerase (New England Biolabs, Beverly, MA, USA), from the respective pJET1.2 plasmids used in yeast transformation (described above), with the following set of primers: CXIP1-F-HindIII, CXIP1-R-BamHI and CXIP2-F-EcoRI, CXIP2-R-BamHI. The sites created for each fragment were *HindIII/BamHI* for *AtGRXS14* and *EcoRI/BamHI* for *AtGRXS16*. The PCR products were then purified using a Nucleospin Gel and PCR Clean up kit (Macherey-Nagel, Duren, Germany), cloned in pGEM-T (pGEM®-T Easy, Promega), and finally cloned into pSAT6.eGFP-N1 vector. For the construction of stable lines of *Arabidopsis* with GFP constructs, the coding regions of *AtSBPs* and *AtGRXS*s with GFP cassette were isolated from pSAT6.eGFP-N1 vector using *Pi-PspI* restriction enzyme and cloned into pPZP-RCS2.nptII binary vector [38].

Multicolour Bimolecular Fluorescence Complementation (BiFC) was carried out with the pSAT vector system [38–40]. *AtSBPs* were isolated as described above using *EcoRI/XmaI* as restriction enzymes and finally cloned into pSAT1.cCFP-N1 vector, in frame with the C-terminus of cCFP (Cyan Fluorescent Protein) protein. *AtGRXS14* and *AtGRXS16* were isolated from pGEM-T vector construct using *HindIII/BamHI* and *EcoRI/BamHI*, respectively, and cloned into pSAT4.nCerulean-N1. For the single transformation in BiFC, coding regions of *AtSBPs* and cCFP cassette were isolated from pSAT1.cCFP-N1 using *Asc-I* restriction enzyme and cloned into pBluescript KS<sup>+</sup>.RCS2 vector, while the coding regions of *AtGRXS*s and the nCerulean cassette were isolated from pSAT4.nCerulean-N1 using *I-SceI* enzyme and finally cloned into pBluescript KS<sup>+</sup>.RCS2, which already contained the coding regions of *AtSBPs* and the cCFP cassette. All constructs were checked by restriction enzyme analysis and sequencing.

## 2.6. Plant transformation

*Agrobacterium tumefaciens* strain GV3101 competent cells were transformed with the proper constructs, using the general freeze-thaw method as described by An et al. [41]. The transformed bacteria were used for the stable transformation of *Arabidopsis* (Col-0) plants via the floral dip method [42].

For *Arabidopsis* protoplast isolation and transfection, the Tape *Arabidopsis*-Sandwich method was used [43]. Protoplasts were isolated from 5-week-old *Arabidopsis* Col-0 rosette leaves, grown under long day conditions. For each transformation experiment 30 µg of plasmid DNA was added to the protoplasts.

## 2.7. Microscopy

The samples were visualized with a Zeiss AxioScope epifluorescence microscope (Zeiss, Oberkochen, Germany), equipped with a Zeiss Axiocam MRc5 digital camera, a differential interference contrast (DIC) system and proper filters. In particular, a filter set with exciter BP450-490 and barrier BP515-595, a set with exciter G-365 and barrier LP420 and a set with exciter BP510-560 and barrier LP590 were used.

## 2.8. Protein molecular modeling and structural prediction of protein-protein interactions

Three dimensional (3D) prediction of Selenium-binding protein 1 (SBP1) from *Arabidopsis thaliana* was generated by using I-TASSER (Iterative Threading ASSEmblY Refinement), an online server that is designed for automated protein structure and function prediction (<https://zhanglab.ccmb.med.umich.edu/ITASSER>), without changing the default parameters of the software [44,45]. The protein sequence of SBP1 from *Arabidopsis thaliana* was retrieved from Uniprot [46] (Accession number O23246). The structural model of SBP1 was constructed from multiple threading alignments and iterative structural assembly simulations. Comparison of the produced models with other known protein structures provides insights for the function of proteins being investigated [47]. Images containing structural models were prepared by the PyMol Molecular Visualization System (<http://www.pymol.org>). Prediction of protein-protein interactions (docking experiments) between SBP1 and CAX-interacting protein 1 (CXIP1) from *Arabidopsis thaliana* were carried out via utilization of the “Prediction Interface” of HADDOCK2.2 web server [48,49]. The 3D structure of SBP1 used in the docking experiment, corresponds to the model constructed by I-TASSER, while in the case of CXIP1 its experimentally determined structure [50] was retrieved from Protein Data Bank [51] (PDB ID: 3IPZ) that corresponds to the mature form of the protein (residues 65 to 173). In order to identify the protein-protein interface residues, the CPORT prediction algorithm was suitably employed on [52]. HADDOCK score, being the weighted sum of inter-molecular electrostatic (Eelec), van der Waals (EvdW), desolvation (ΔGsolv) and ambiguous interaction restraint (AIR) energies, was used to rank the generated poses. The resulted models were visualized with the PyMol Molecular Visualization System. Calculations of the properties of the interfaces of the interacting proteins were carried out utilizing PISA software [53].

## 3. Results and discussion

### 3.1. Isolation of AtGRXS14 (AtGRXcp or AtCXIP1) as an interacting protein of AtSBP1 and sequence analysis of AtGRXS14

To study the function of SBP in plants we screened an *A. thaliana* cDNA library for potential interacting proteins of SBP1 using the yeast two hybrid system. Amongst the clones we identified in this manner was AtGRXS14, known at the time of the experiment as AtCXIP1 [23].

AtGRXS14 (NP\_191050) constitutes a protein of 173 aa (Fig. 1A). It

contains a GRX PICOT-like domain between aa 74–164 (indicated by a grey arrow) and a GSH binding domain (within the PICOT) (Fig. 1A). AtGRXS14 shares 20% identity, particularly in the PICOT domain region, with AtGRXS16 (or AtCXIP2) (NP\_565885) (Fig. 1B), a 293 aa protein. The alignment of the two proteins is shown in Fig. 1C and a graphical domain overview alignment in Fig. 1D.

AtGRXS14 and AtGRXS16 are both plastidial class II GRXs, possessing dual in vitro biochemical functions, namely reductase and Fe-S cluster ligase activity [22].

Several proteins that contain a PICOT-HD also contain a Trx-HD, including *Arabidopsis* AtGRXS16. Proteins containing the Trx-HD are important in a range of cellular process, including controlling the redox state of the cell [23,54]. The human PICOT protein is involved in the interaction with protein kinase C through this Trx-HD and negatively regulates the c-Jun N-terminal kinase/AP-1 and NF- $\kappa$ B pathway [55]. AtGRXS14 is 43% similar to AtGRXS16 overall and is 54% identical to AtGRXS16 within the PICOT-HD. Human PICOT has been characterized as an iron-sulfur (Fe/S) protein [56], similar to the PICOT homolog in yeast, Grx3, which was shown to play a crucial role in intracellular iron trafficking and sensing [57]. Iron-sulfur proteins are ubiquitously expressed and participate in diverse biochemical functions in virtually every living cell. They consist of two or more iron atoms bridged by sulfur ligands and are involved in diverse processes, including respiration, oxidation-reduction reactions, heme biosynthesis, iron homeostasis, and regulation of gene expression [58].

### 3.2. AtSBP protein family interactions with AtGRXS14 and AtGRXS16

The identification of protein-protein interactions comprises a prerequisite towards understanding protein networks and functions, as proteins normally function in macromolecular complexes. Describing such interactions, although it may be of great interest, it can be challenging, since they may be transient, or may involve different partners and overlapping binding sites [59].

In order to verify the positive interaction of AtGRXS14 with AtSBP1 revealed by the yeast two-hybrid (Y2H) screening (with AtSBP1 as bait), the respective genes were amplified from total *Arabidopsis* root RNA and cloned in appropriate vectors and individual protein-protein interaction experiments were performed. Additionally, *AtSBP2*, *AtSBP3* and *AtGRXS16* were also amplified and cloned due to their high degree of homology with the bait and prey proteins, respectively (Supplementary Fig. 1, Fig. 1). Due to the highly conserved nature of selenium binding proteins and glutaredoxins we also attempted to utilize the human homologue of SBP1 in interaction assays with the plant glutaredoxins and therefore HsSBP1 was amplified from human cDNA and cloned in frame with the GAL4 activation domain.

Yeast cells coexpressing various construct combinations in pairs, were used to study protein-protein interactions (Fig. 2A). This assay confirmed initially a strong positive interaction of AtGRXS14 with AtSBP1 and a weaker one with AtSBP3. Interestingly, all three AtSBP proteins also strongly interacted with AtGRXS16. These interactions were revealed by the choice we made to test the particular pairs, based on the significant homology of AtGRXS14 and AtGRXS16 within the PICOT domain, since AtGRXS16 was not identified as an interacting partner in the Y2H screening. It is noteworthy, that HsSBP1 physically binds to AtGRXS16, in a weak manner though, demonstrating a presumed functionally conserved protein network. No unspecific activation was detected when bait and prey proteins were used in combination with the respective empty vectors (pGBKT7 or pGADT7).

Our data point to the existence of a novel protein-protein interaction network, consisting of the selenium binding protein family and the plastidial glutaredoxins AtGRXS14 and AtGRXS16, where AtGRXS14 specifically binds AtSBP1, while AtGRXS16 binds to all three SBP members. Taking into account the properties and the suggested functions of the participating proteins, it is plausible to speculate that this network is part of the plant's response to oxidative stress.

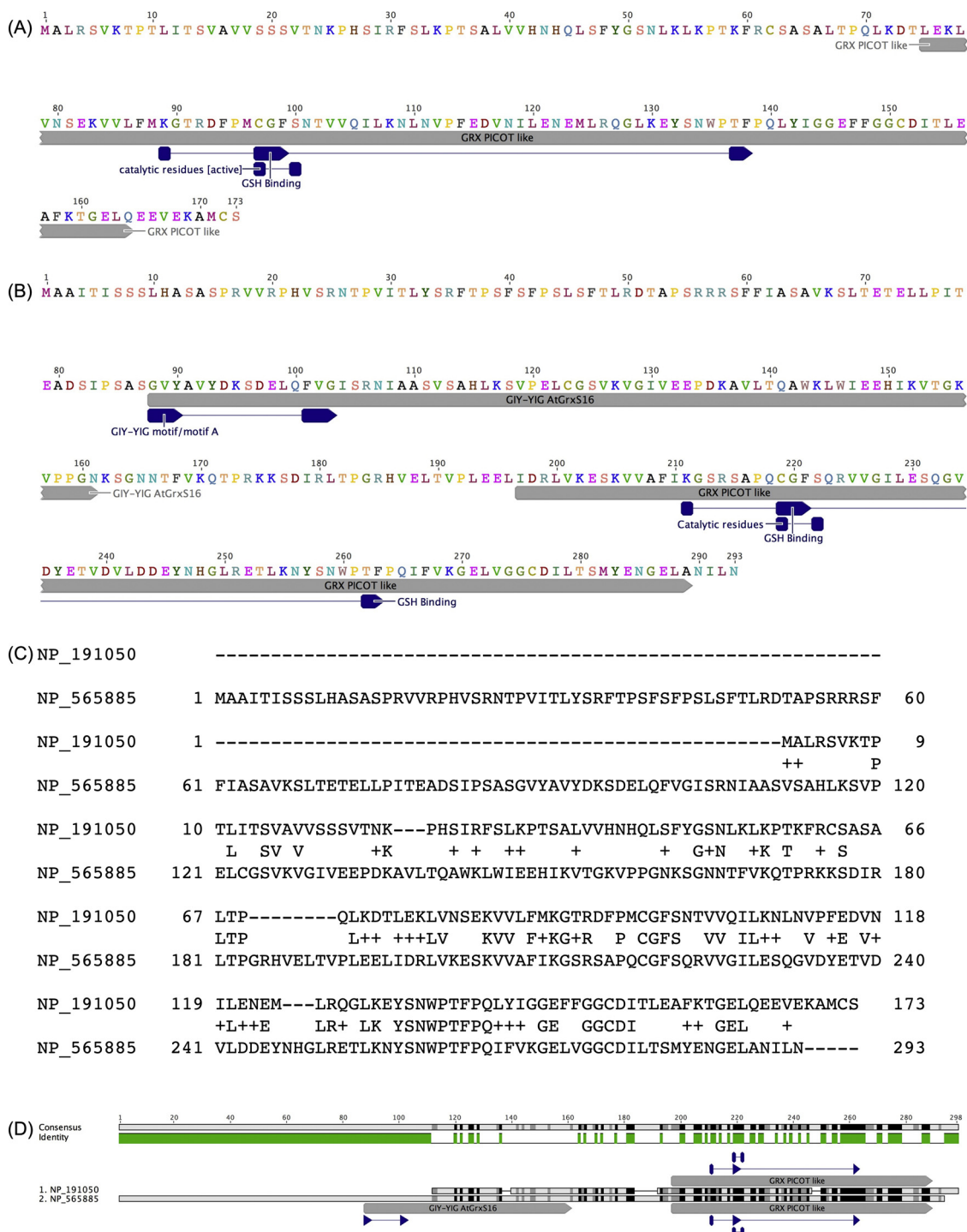


**Fig. 1. Sequence characteristics of AtGRXS14 and AtGRXS16.** (A) and (B) amino acid sequence of AtGRXS14 and AtGRXS16 respectively. The PICOT-like domains are shown as gray bars and the catalytic residues along with the GSH binding sites are shown as blue boxes. (C) Amino acid sequence comparison of AtGRXS14 and AtGRXS16. A significant degree of conservation is observed within the PICOT domain towards the carboxy terminal. (D) Graphical alignment of the annotated domains of AtGRXS14 and AtGRXS16 (For interpretation of the references to colour in this figure legend, the reader is referred to the web version of this article).

Moreover, we tried to determine domains in the AtSBP1 polypeptide, responsible for binding of AtGRXS14. We generated a series of C-terminal truncated AtSBP1 polypeptides (Fig. 2E) and studied in yeast cells their binding capacity to AtGRXS14. Firstly, we investigated whether these truncated polypeptides cloned in frame with the binding domain of GAL4 react in an unspecific manner with the activation domain of the empty vector (Fig. 2B). Indeed, we demonstrated that this was the case for the first 53 aa of AtSBP1 (AtSBP1DEL8). On the contrary, when we swapped domains and AtSBP1DEL8 was fused to the

activation domain of GAL4 no unspecific growth was detected with the binding domain of the empty vector (pGBKT7) (Fig. 2B). We then analyzed the auxotrophy of yeast cells while harboring in pairs AtGRXS14 and each of the eight truncated polypeptides of AtSBP1 (Fig. 2C). Our analysis showed that the first 178 aa of AtSBP1 maintain strong, full binding capacity to AtGRXS14, while the region between aa 358–427, when deleted, interferes with proper binding. We believe that the behavior of constructs AtSBP1DEL2 and AtSBP1DEL3 is due to conformational changes that might occur to the truncated protein,

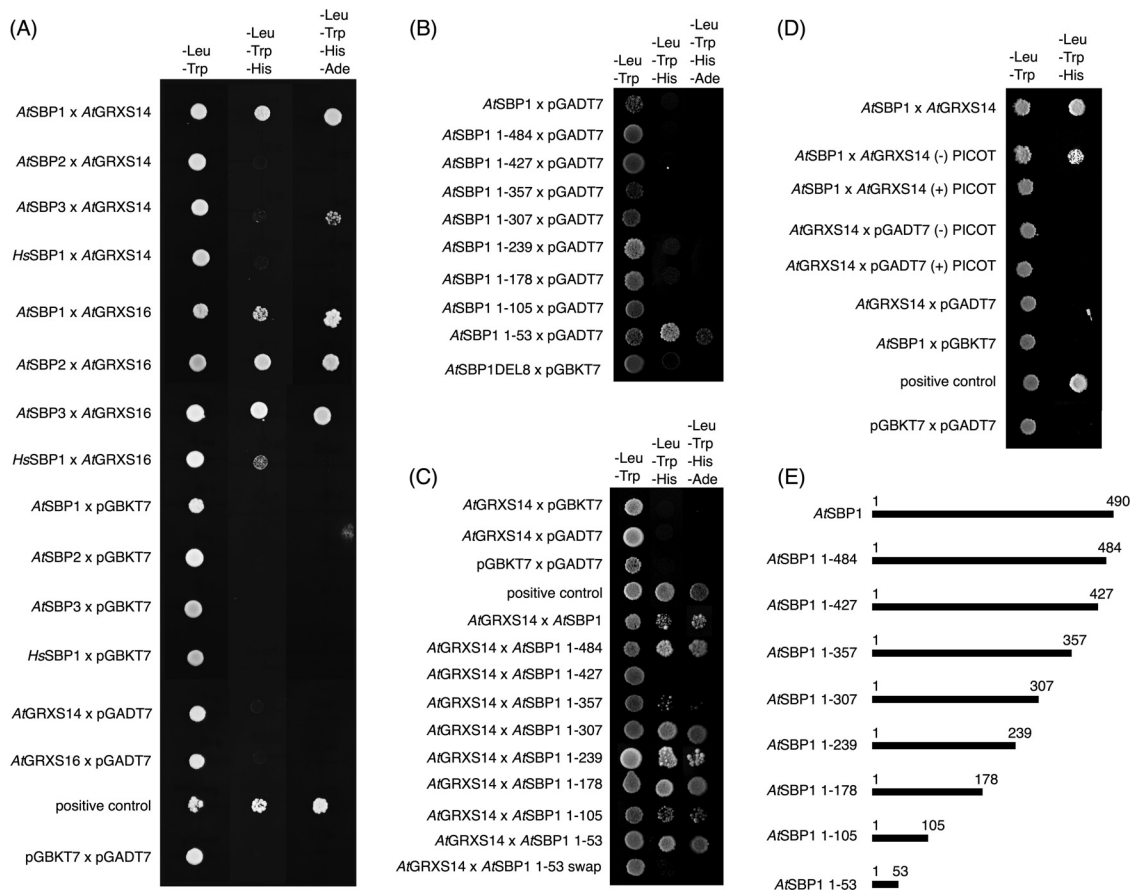


**Fig. 2.** Yeast two-hybrid assays. (A) Confirmation that AtGRXS14 from the yeast two-hybrid screening interacts with the bait protein AtSBP1. Furthermore, AtGRXS16 interacts with all members of the SBP protein family. A weak interaction of the human SBP1 with AtGRXS16 was also observed. Proper controls to exclude unspecific vector activation were included along with the 53/T positive control. (B) Evaluation of the effect of the GAL4 activation domain (AD) in terms of false positive appearance. The AD of the empty vector unspecifically binds to the truncated version of AtSBP1, AtSBP1DEL8. Immediately below this interaction the same truncated version of AtSBP1 is shown, after domain swapping. (C) Deletion analysis of AtSBP1. The shortest truncated version of AtSBP1 that interacts with AtGRXS14 is AtSBP1DEL7 of 105 N-terminal aminoacids. (D) AtSBP1 does not bind the PICOT domain of AtGRXS14. The interaction of AtGRXS14 with AtSBP1 is confined to N-terminal half of AtGRXS14 that does not contain the PICOT domain. Proper negative and positive controls were included. (E) The truncated polypeptides of AtSBP1 used for deletion analysis in (C). The relative position of the last aminoacid in each deletion is indicated by a number.

resulting in a folding arrangement that interferes with proper binding of GRXS14 to SBP1.

PICOT-HD is a highly conserved protein domain that is often associated with thioredoxin and glutaredoxin modules [60]. Therefore, we asked if the PICOT domain of AtGRXS14 is directly involved in AtSBP1 binding. We prepared two truncated versions of AtGRXS14 with and without the PICOT domain and translationally fused them to the binding domain of GAL4. These polypeptides comprised of aa 1–82 and 83–173 respectively, the latter containing only the PICOT domain. These constructs were transferred to yeast cells along with AtSBP1 fused to GAL4 activation domain and the relative strains were tested for auxotrophy (Fig. 2D). Our data showed that AtSBP1 interacts with the N-terminal region of AtGRXS14 upstream of the PICOT domain.

### 3.3. Docking experiments

Results from yeast two-hybrid (Y2H) screening regarding the AtSBP1-AtGRXS14 complex reveal the significance of the residues located at the N-terminus of AtSBP1 in order interaction between them to be achieved. They also indicate that truncated sequences of AtSBP1 fail to interact with AtGRXS14 in a proper manner, suggesting that the full sequence of AtSBP1 is necessary for the formation of the complex.

In order to predict the mode of interaction between AtSBP1 and AtGRXS14 in *Arabidopsis thaliana*, driven docking experiments were performed utilizing the HADDOCK2.2 Web Server. Since the three-

dimensional structure of AtSBP1 has not been experimentally determined a theoretical model of the protein was constructed by I-TASSER server, providing as input the sequence of AtSBP1 from Uniprot. In order to estimate the quality of the predicted model by I-TASSER, the C-score was calculated. C-score is a confidence score that its value typically ranges from -5 to +2. A high value of C-score indicates high confidence in the model. The predicted model was also evaluated utilizing both the template modeling-score (TM-score) and the root mean-square difference (RMSD). TM-score corresponds to a scale for measuring the structural similarity between two proteins with different tertiary structures. A value of TM-score over +0.5 indicates that the topology of the predicted model is correct, while a value below +0.17 indicates random similarity. In our case, the values of C-score, TM-score and RMSD for the predicted model are -0.02,  $0.71 \pm 0.12$  and  $7.3 \pm 4.2 \text{ \AA}$ , respectively. These values indicate that our predicted model is reliable in order to be used in subsequent docking experiments with the exception of residues 1 to 23 at the N terminus of the protein. This is due to the fact that there is no proper template available that can be used to model that part. A detailed observation of the resulted model indicates the abundance of beta-strands that form a seven-blade beta-propeller surrounded by  $\alpha$ -helices (Fig. 3A). The overall structure is in agreement with previously reported structural models of SBP1 from *Arabidopsis thaliana* [33] and *Homo sapiens* [61] that were produced by the homology modeling method. This is due to the fact that in all cases the template structure used, was the hypothetical selenium-binding

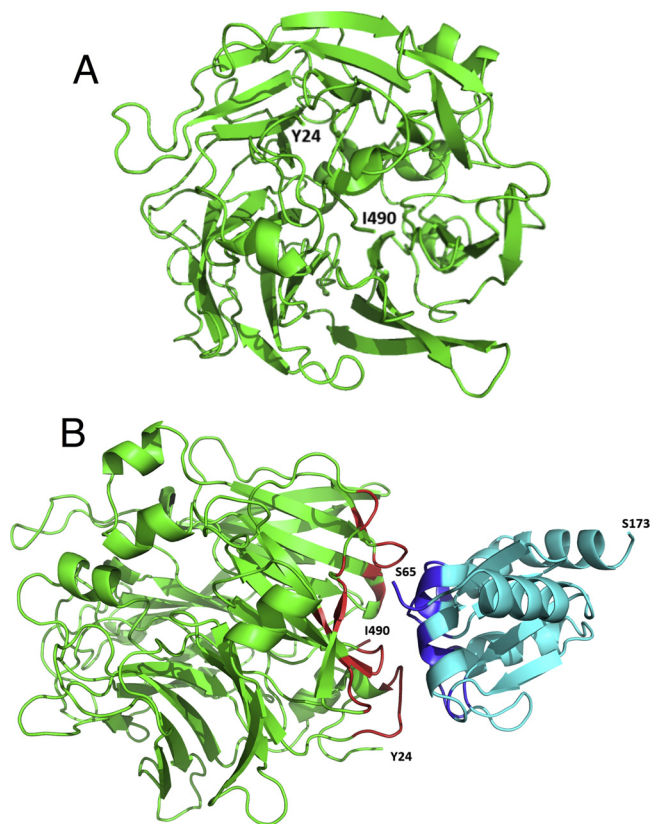


**Fig. 3.** A ribbon model of AtSBP1 structure and a representation of the predicted AtSBP1-AtGRXS14 complex. (A) A ribbon model of AtSBP1 structure (colored in green), displayed using the software PyMOL. The overall structure of AtSBP1 is comprised of a seven-blade beta-propeller surrounded by  $\alpha$ -helices. (B) A cartoon representation of the predicted AtSBP1-AtGRXS14 complex (colored in green and cyan, respectively), displayed using the software PyMOL. The interfacing residues, calculated by PISA, are colored red (AtSBP1) and blue (AtGRXS14), respectively (For interpretation of the references to colour in this figure legend, the reader is referred to the web version of this article).

protein from *Sulfolobus tokodaii* (PDB ID: 2ECE) resulting in models with very similar structural features.

On the other hand, the structure of AtGRXS14 is experimentally determined by X-ray Crystallography (PDB ID: 3IPZ) [3]. The deposited structure corresponds to the mature form of the protein (residues 65–173) while residues 1–63 form a signal peptide that targets the protein to the chloroplast. It adopts a glutaredoxin/thioredoxin-like fold that consists of a four-stranded parallel  $\beta$ -sheet surrounded by five  $\alpha$ -helices [50].

For the prediction of the protein-protein interface residues that will be provided subsequently as input to the HADDOCK2.2 Web Server, the CPORT algorithm was used. The driven docking experiment provided a solution (Fig. 3B) that exhibited a HADDOCK score of -136.4, with the values of energies (Kcal/mole) having been calculated as following: (a) van der Waals energy: -36.2; (b) electrostatic energy: -375.2; (c) desolvation energy: -48.5; (d) restraints violation energy: 233.7 and (e) total buried surface area (BSA): 1667.5  $\text{\AA}^2$ . It must be noted that the high value of restraints violation energy is due to the fact that a large number of residues that were considered as active by the CPORT algorithm were not taken into account during the docking experiment. The residues that participate in the interface between AtSBP1 and AtGRXS14 were calculated with PISA software. In the case of AtSBP1 these residues are 101–106, 160–163, 182, 184–186, 191–192, 194, 196–197, 212, 214, 250–252, 254 and 490 while in AtGRXS14 these are 65–66, 89, 96–99, 120, 126–127, 130–131, 134–138 and 152. The

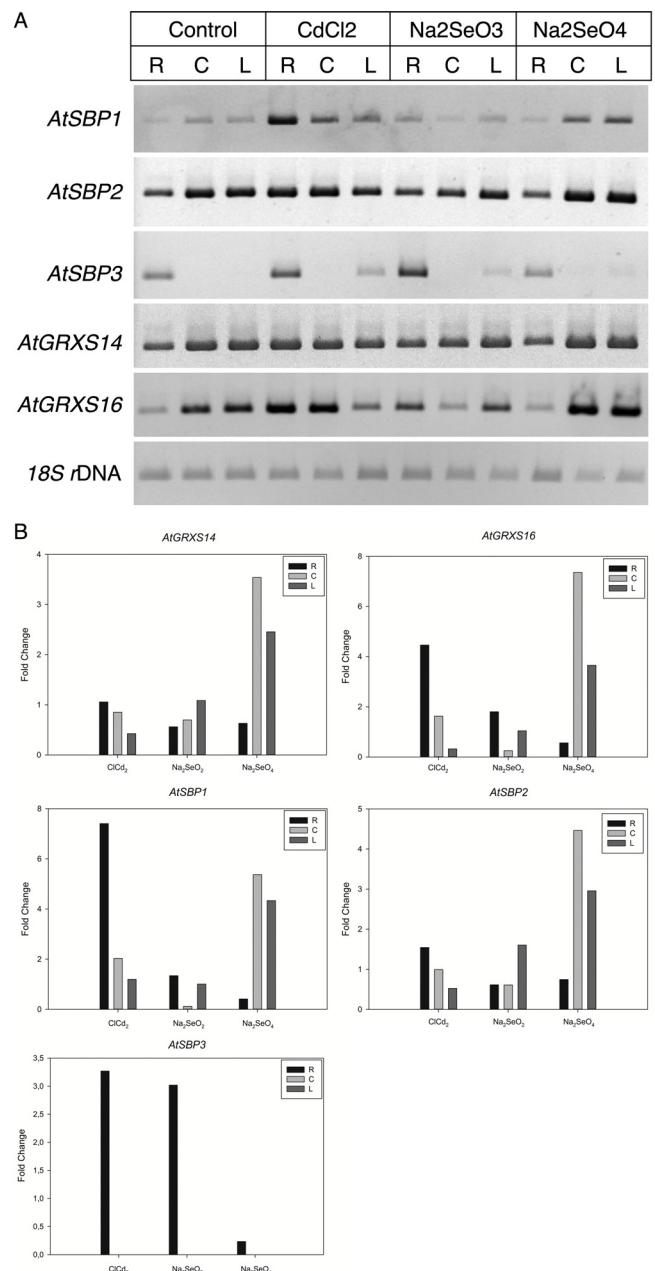


**Fig. 4.** RT-PCR analysis of SBP genes, AtGRXS14 and AtGRXS16 upon treatment with oxidative stress inducers. (A) Plants were treated with 150  $\mu\text{M}$  CdCl<sub>2</sub>, Na<sub>2</sub>SeO<sub>3</sub> and Na<sub>2</sub>SeO<sub>4</sub> and transcript levels were compared to untreated control plants. Samples were normalized with the housekeeping 18S rDNA. (R) Roots, (C) Cotyledons, (L) Leaves. The PCR cycles were as follows: SBP1(28), SBP2(35), SBP3(35), GRXS14(33), GRXS16(33), 18S(26). (B) Bar charts depicting expression levels of genes studied, following densitometric analysis of the bands presented in (A). Differences in gene expression are shown as fold-change over the control after normalization with the housekeeping 18S rDNA. (R) Roots, (C) Cotyledons, (L) Leaves.

complex is stabilized by a network of hydrogen bonds, that is formed between the interfacing residues of these two proteins. Moreover, residues Asp103, Glu163 and Lys214 from AtSBP1 form salt bridges with residues Lys89, Lys130 and Asp152 from AtGRXS14, respectively.

Consequently, the results of the docking experiment strongly support the experimental results showing the significance of the N-terminus of AtSBP1 for the interaction with AtGRXS14 and they, additionally, stress the role of the full sequence of AtSBP1 in the interaction, since the C-terminus (residue 490) is also part of the

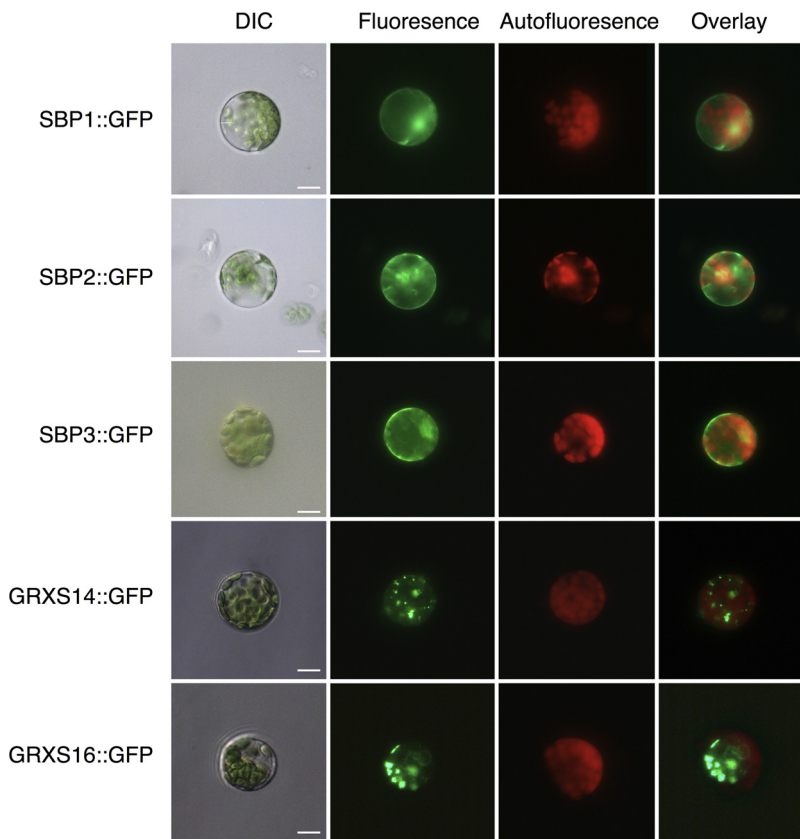


**Fig. 5. Transient expression assays in Arabidopsis protoplasts.** The genes of interest were fused to GFP to generate the chimeric constructs indicated on the left of the panel. SBP proteins were localized in the cytoplasm and the nucleus. AtGRXS14 localized in speckle-like structures associated with the chloroplasts and AtGRXS16 in the chloroplast body. Cells were visualized under an epifluorescence microscope equipped with DIC optics and GFP filter sets. Bars 25  $\mu$ m.

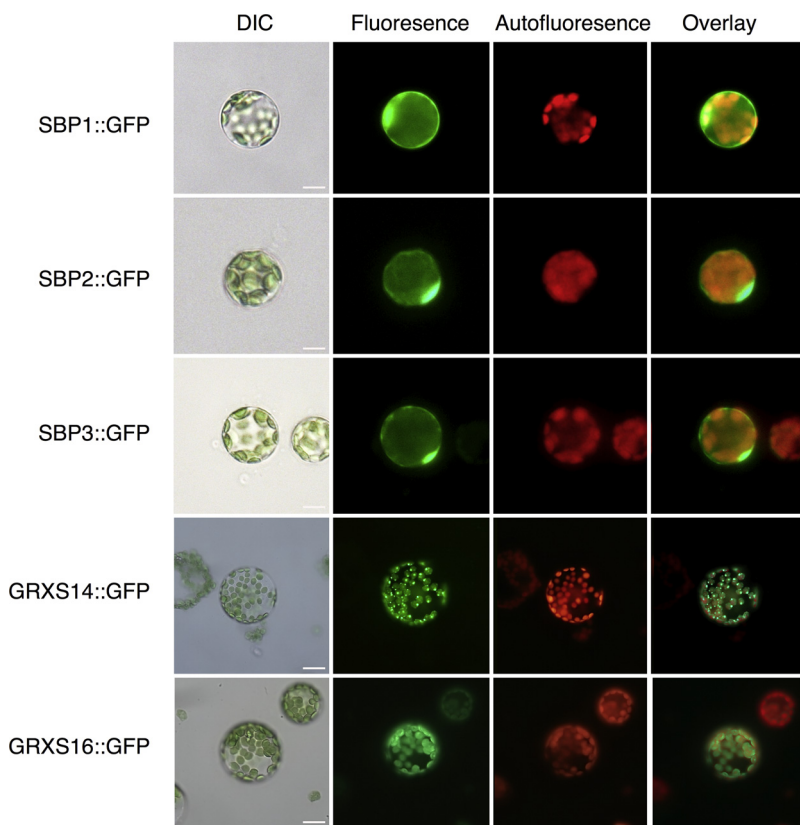


**Fig. 6. Transgenic protoplasts from stably transformed Arabidopsis plants.** Chimeric constructs indicated on the left of the panel were used to stably transform plants via *Agrobacterium*-mediated transformation. Rosette protoplasts were assayed for GFP expression. SBP proteins were localized in the cytoplasm and the nucleus. AtGRXS14 localized in speckle-like structures associated with the chloroplasts and AtGRXS16 in the chloroplast body. Cells were visualized under an epifluorescence microscope equipped with DIC optics and GFP filter sets. Bars 25  $\mu$ m.

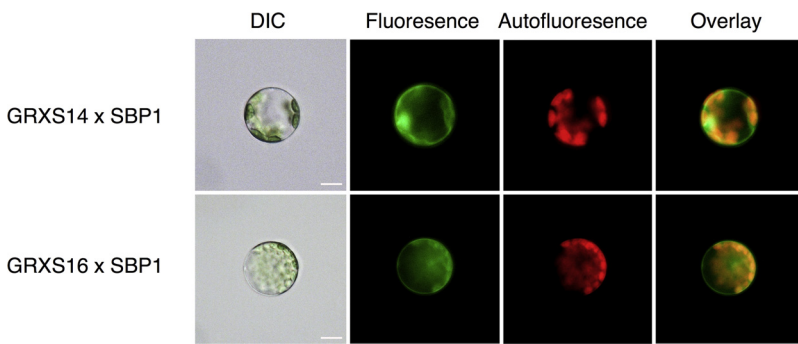


**Fig. 7. BiFC in Arabidopsis protoplasts.** AtSBP1 interacts *in planta* with AtGRXS14 in the nucleus and the cytoplasm while the interaction signal with AtGRXS16 is confined in the cytoplasm only. Cells were visualized under an epifluorescence microscope equipped with DIC optics and GFP filter sets. Bars 25  $\mu$ m. Negative controls were included (Supplementary Fig. 2).

predicted interface.

Based on the fact that certain residues of AtGRXS14 like Lys89, Lys130 and Asp152 are involved in GSH binding, one could speculate that GSH competes with AtGRS14 for binding to AtSBP1, since Dutilleul et al. [27] have provided evidence that SBP1 protein can function in Cd detoxification, acting in parallel with GSH and phytochelatin.

#### 3.4. Gene expression analysis of AtSBP family, AtGRXS14 and AtGRXS16

Since *AtSBP* gene family is differentially regulated by sodium selenite and sodium selenate [35] and *AtSBP1* is upregulated by cadmium [27,34] it would be interesting to determine the relative transcript accumulation of *AtGRXS14* and *AtGRXS16* after treatment of plants with the aforementioned compounds (Fig. 4). Therefore, we investigated the gene expression patterns of the *AtSBP* gene family and those of *AtGRXS14* and *AtGRXS16* in control plants, as well as, in response to cadmium and selenium compounds.

*AtSBP1* is strongly induced by 150  $\mu$ M CdCl<sub>2</sub> in the roots and marginally upregulated in cotyledons and leaves of 10-day-old plants, after treatment with 150  $\mu$ M Na<sub>2</sub>SeO<sub>4</sub>. *AtSBP2* is constitutively expressed under all treatments. *AtSBP3* is expressed only in the roots of untreated plants and it is induced in roots and leaves after CdCl<sub>2</sub> and Na<sub>2</sub>SeO<sub>3</sub> treatment. *AtGRXS14*, like *AtSBP2*, is constitutively expressed under all conditions tested. *AtGRXS16* transcript accumulates at higher levels in the cotyledons and leaves of untreated plants. Upon treatment with CdCl<sub>2</sub> it is highly induced in the roots with an approximate two-fold induction in the cotyledons. From the two selenium compounds tested only Na<sub>2</sub>SeO<sub>4</sub> treatment leads to the upregulation of *AtGRXS16* in cotyledons and leaves. The reason why we included *AtGRXS16* in this analysis was that *AtGRXS16* interacted in yeast with the members of the AtSBP protein family.

Concerning the *AtSBP* family, the expression patterns observed are, generally, in line with previous studies [29,34,35], but we show additionally that also *AtSBP3* participates in the network of genes upregulated in response to CdCl<sub>2</sub> and Na<sub>2</sub>SeO<sub>3</sub>. Overall, these data further strengthen previous observations that indeed *AtSBP* gene family is differentially regulated by cadmium, selenite and selenate.

In *Arabidopsis thaliana*, it has been shown that, oxidative stress due to cadmium exposure relates to hydrogen peroxide accumulation [62] and that treatment of plants with selenium compounds led to ROS accumulation in the roots [35]. It has also been proposed, that in addition to the importance of SBP1 in stress responses, SBP2 and SBP3, along with SBP1, constitute integrated components of a network that responds to the cellular redox state [35]. Furthermore, studies using plate-grown plantlets and leaf discs have implicated GRXS14 and GRXS16 in oxidative stress responses [24,63], while GRXS14 deficiency results in the reduction of chlorophyll content in dark and its overexpression is correlated with both altered chlorophyll content and reduced amounts of NFU2, a scaffold protein required for [4Fe-4S] and ferredoxin iron-sulphur cluster assembly [22,64]. Taken together the above and considering the interactions of AtGRXS14 and AtGRXS16 with the members of the AtSBP protein family (see below), it is

tempting to speculate that this gene and/or protein network functions in a concerted manner in response to oxidative stress.

#### 3.5. Subcellular localization and in-planta interactions

It has been reported previously that the human SBP1 localizes in the cytosol and the nucleus [65–67], while studies in plants demonstrated the expression of SBP in cytoplasmically dense cell types and membrane vesicles [28]. In order to elucidate in which cellular compartments our proteins of interest are localized, we initially performed transient expression assays in Arabidopsis protoplasts. AtSBPs, AtGRXS14 and AtGRXS16 were translationally fused to GFP and used to transform rosette leaf protoplasts (Fig. 5). This analysis showed that SBP protein fusions can be present both in the cytoplasm and the nucleus, while the respective AtGRXS14 and AtGRXS16 fusions relate to the chloroplasts. Interestingly, AtGRXS14 localized in speckle-like structures, whereas the AtGRXS16 derived signal was evenly distributed in the chloroplast body.

To further enhance the detail of our observations we utilized protoplasts from plants stably transformed with the GFP fusions (Fig. 6). The expression patterns observed with transient assays were confirmed in a clearer manner but in the case of AtGRXS14 it became evident that intense signal is formed in the chloroplast and usually in one speckle-like structure associated with it.

The chloroplastic localization of the *Populus trichocarpa* GrxS14 and GrxS16 has also been shown in the heterologous system of tobacco leaves by transient expression assays [68], where GFP fusions were expressed in the guard cells of the stomata. Furthermore, AtGRXS16-GFP was transiently expressed in tobacco mesophyll cells and localized in the chloroplasts [69]. Our data are in line with the aforementioned studies, but they also reveal in the homologous Arabidopsis system a new expression pattern, as far as AtGRXS14 is concerned.

We then asked if the interactions revealed by the yeast two-hybrid screening occur *in planta*. To answer this question we employed bimolecular fluorescence complementation (BiFC) to probe the protein interactions in living protoplast cells [40,70]. Arabidopsis protoplasts were transiently transformed with constructs of the interacting pairs in the pSAT vector system [39,40]. As shown in Fig. 7, AtSBP1 interacts *in planta* with AtGRXS14 in the nucleus and the cytoplasm while the interaction signal with AtGRXS16 is confined in the cytoplasm only.

Our subcellular localization analyses define for the first time the compartmentalized expression pattern of the AtSBP protein family and reveal in a homologous system a novel pattern for AtGRXS14 (Fig. 5). Furthermore, we show that probably prior to their translocation to the chloroplast AtGRXS14 and AtGRXS16 are retained in the cytoplasm to interact with AtSBP1 (and even in the nucleus in the case of AtGRXS14) (Fig. 7), when ectopically expressed. It is known that certain cytosolic factors such 14-3-3 protein, Hsp70, Hsp90 and FKBP bind to particular peptides and are thought to facilitate protein targeting to the chloroplasts [71–73]. It remains unclear and worth further investigation under which conditions the described interactions occur *in vivo*.

## Conflict of interest statement

The authors declare that the research was conducted in the absence of any commercial or financial relationships that could be construed as a potential conflict of interest.

## Acknowledgements

This work was supported by the NKUA Special Account for Research Grants (S.A.R.G.). Irene Dervisi was supported by the Greek State Scholarships Foundation (IKY).

## Appendix A. Supplementary data

Supplementary material related to this article can be found, in the online version, at doi:<https://doi.org/10.1016/j.plantsci.2019.01.021>.

## References

- [1] B. Halliwell, Reactive species and antioxidants. Redox biology is a fundamental theme of aerobic life, *Plant Physiol.* 141 (2006) 312–322.
- [2] B. Halliwell, J.M.C. Gutteridge, *Free Radicals in Biology and Medicine*, Clarendon Press, 1985.
- [3] O. Blokhina, K.V. Fagerstedt, Reactive oxygen species and nitric oxide in plant mitochondria: origin and redundant regulatory systems, *Physiol. Plant.* 138 (2010) 447–462.
- [4] E. Heyno, V. Mary, P. Schopfer, A. Krieger-Liszak, Oxygen activation at the plasma membrane: relation between superoxide and hydroxyl radical production by isolated membranes, *Planta* 234 (2011) 35–45.
- [5] K. Shah, R.G. Kumar, S. Verma, R.S. Dubey, Effect of cadmium on lipid peroxidation, superoxide anion generation and activities of antioxidant enzymes in growing rice seedlings, *Plant Sci.* 161 (2001) 1135–1144.
- [6] R. Desikan, S. A-H-Mackerness, J.T. Hancock, S.J. Neill, Regulation of the Arabidopsis transcriptome by oxidative stress, *Plant Physiol.* 127 (2001) 159–172.
- [7] S. Neill, R. Desikan, J. Hancock, Hydrogen peroxide signalling, *Curr. Opin. Plant Biol.* 5 (2002) 388–395.
- [8] J. Yan, N. Tsuchihara, T. Etoh, S. Iwai, Reactive oxygen species and nitric oxide are involved in ABA inhibition of stomatal opening, *Plant Cell Environ.* 30 (2007) 1320–1325.
- [9] R. Mittler, S. Vanderauwera, M. Gollery, F. Van Breusegem, Reactive oxygen gene network of plants, *Trends Plant Sci.* 9 (2004) 490–498.
- [10] M.C. Rentel, D. Lecourieux, F. Ouaked, S.L. Usher, L. Petersen, H. Okamoto, H. Knight, S.C. Peck, C.S. Grierson, H. Hirt, M.R. Knight, OX1 kinase is necessary for oxidative burst-mediated signalling in Arabidopsis, *Nature* 427 (2004) 858–861.
- [11] D. Gollack, C. Li, H. Mohan, N. Probst, Tolerance to drought and salt stress in plants: unraveling the signaling networks, *Front. Plant Sci.* 5 (2014) 151.
- [12] A.P. Fernandes, M. Fladvad, C. Berndt, C. Andresen, C.H. Lillig, P. Neubauer, M. Sunnerhagen, A. Holmgren, A. Vlamis-Gardikas, A novel monothiol glutaredoxin (Grx4) from *Escherichia coli* can serve as a substrate for thioredoxin reductase, *J. Biol. Chem.* 280 (2005) 24544–24552.
- [13] Y. Meyer, B.B. Buchanan, F. Vignols, J.P. Reichheld, Thioredoxins and glutaredoxins: unifying elements in redox biology, *Annu. Rev. Genet.* 43 (2009) 335–367.
- [14] N. Rouhler, E. Gelhaye, J.P. Jacquot, Plant glutaredoxins: still mysterious reducing systems, *Cell. Mol. Life Sci.* 61 (2004) 1266–1277.
- [15] N. Rouhler, S.D. Lemaire, J.P. Jacquot, The role of glutathione in photosynthetic organisms: emerging functions for glutaredoxins and glutathionylation, *Annu. Rev. Plant Biol.* 59 (2008) 143–166.
- [16] J. Couturier, J.P. Jacquot, N. Rouhler, Evolution and diversity of glutaredoxins in photosynthetic organisms, *Cell. Mol. Life Sci.* 66 (2009) 2539–2557.
- [17] Y. Meyer, W. Siala, T. Bashandy, C. Riondet, F. Vignols, J.P. Reichheld, Glutaredoxins and thioredoxins in plants, *Biochim. Biophys. Acta* 1783 (2008) 589–600.
- [18] S. Xing, A. Lauri, S. Zachgo, Redox regulation and flower development: a novel function for glutaredoxins, *Plant Biol. (Stuttg.)* 8 (2006) 547–555.
- [19] N.H. Cheng, J.Z. Liu, X. Liu, Q. Wu, S.M. Thompson, J. Lin, J. Chang, S.A. Whitham, S. Park, J.D. Cohen, K.D. Hirschi, Arabidopsis monothiol glutaredoxin, AtGRXS17, is critical for temperature-dependent postembryonic growth and development via modulating auxin response, *J. Biol. Chem.* 286 (2011) 20398–20406.
- [20] L. Hong, D. Tang, K. Zhu, K. Wang, M. Li, Z. Cheng, Somatic and reproductive cell development in rice anther is regulated by a putative glutaredoxin, *Plant Cell* 24 (2012) 577–588.
- [21] C. Riondet, J.P. Desouris, J.G. Montoya, Y. Chartier, Y. Meyer, J.P. Reichheld, A dicotyledon-specific glutaredoxin GRXC1 family with dimer-dependent redox regulation is functionally redundant with GRXC2, *Plant Cell Environ.* 35 (2012) 360–373.
- [22] P. Rey, N. Becuwe, S. Tourrette, N. Rouhler, Involvement of Arabidopsis glutaredoxin S14 in the maintenance of chlorophyll content, *Plant Cell Environ.* 40 (2017) 2319–2332.
- [23] N.H. Cheng, K.D. Hirschi, Cloning and characterization of CXIP1, a novel PICOT domain-containing Arabidopsis protein that associates with CAX1, *J. Biol. Chem.* 278 (2003) 6503–6509.
- [24] N.H. Cheng, J.Z. Liu, A. Brock, R.S. Nelson, K.D. Hirschi, AtGRXcp, an Arabidopsis chloroplastic glutaredoxin, is critical for protection against protein oxidative damage, *J. Biol. Chem.* 281 (2006) 26280–26288.
- [25] A. Agalou, H.P. Spaink, A. Roussis, Novel interaction of selenium-binding protein with glyceraldehyde-3-phosphate dehydrogenase and fructose-bisphosphate aldolase of Arabidopsis thaliana, *Funct. Plant Biol.* 33 (2006) 847–856.
- [26] A. Agalou, A. Roussis, H.P. Spaink, The Arabidopsis selenium-binding protein confers tolerance to toxic levels of selenium, *Funct. Plant Biol.* 32 (2005) 881–890.
- [27] C. Dutilleul, A. Jourdain, J. Bourguignon, V. Hugouvieux, The Arabidopsis putative selenium-binding protein family: expression study and characterization of SBP1 as a potential new player in cadmium detoxification processes, *Plant Physiol.* 147 (2008) 239–251.
- [28] E. Fletmetakis, A. Agalou, N. Kavroulakis, M. Dimou, A. Martsikovskaya, A. Slater, H.P. Spaink, A. Roussis, P. Katinakis, Lotus japonicus gene Ljsbp is highly conserved among plants and animals and encodes a homologue to the mammalian selenium-binding proteins, *Mol. Plant Microbe Interact.* 15 (2002) 313–322.
- [29] V. Hugouvieux, C. Dutilleul, A. Jourdain, F. Reynaud, V. Lopez, J. Bourguignon, Arabidopsis putative selenium-binding protein1 expression is tightly linked to cellular sulfur demand and can reduce sensitivity to stresses requiring glutathione for tolerance, *Plant Physiol.* 151 (2009) 768–781.
- [30] K. Sawada, M. Hasegawa, L. Tokuda, J. Kameyama, O. Kodama, T. Kohchi, K. Yoshida, A. Shinmyo, Enhanced resistance to blast fungus and bacterial blight in transgenic rice constitutively expressing OsSBP, a rice homologue of mammalian selenium-binding proteins, *Biosci. Biotechnol. Biochem.* 68 (2004) 873–880.
- [31] K. Sawada, M. Iwata, Isolation of blast fungal cerebroside elicitor-responsive genes in rice plants, *J. Gen. Plant Pathol.* 68 (2002) 128–133.
- [32] K. Sawada, L. Tokuda, A. Shinmyo, Characterization of the rice blast fungal elicitor-responsive gene OsSBP encoding a homolog to the mammalian selenium-binding proteins, *Plant Biotechnol.* 20 (2003) 177–181.
- [33] F. Schild, S. Kieffer-Jaquinod, A. Palencia, D. Cobessi, G. Sarret, C. Zubieta, A. Jourdain, R. Dumas, V. Forge, D. Testemale, J. Bourguignon, V. Hugouvieux, Biochemical and biophysical characterization of the selenium-binding and reducing site in Arabidopsis thaliana homologue to mammalian selenium-binding protein 1, *J. Biol. Chem.* 289 (2014) 31765–31776.
- [34] J.E. Sarry, L. Kuhn, C. Ducruix, A. Lafaye, C. Junot, V. Hugouvieux, A. Jourdain, O. Bastien, J.B. Fievet, D. Vailhen, B. Amekraz, C. Moulin, E. Ezan, J. Garin, J. Bourguignon, The early responses of Arabidopsis thaliana cells to cadmium exposure explored by protein and metabolite profiling analyses, *Proteomics* 6 (2006) 2180–2198.
- [35] C. Valassakis, P. Livanos, M. Minopetrou, K. Haralampidis, A. Roussis, Promoter analysis and functional implications of the selenium binding protein (SBP) gene family in Arabidopsis thaliana, *J. Plant Physiol.* 224–225 (2018) 19–29.
- [36] G.M. Lacourciere, R.L. Levine, T.C. Stadman, Direct detection of potential selenium delivery proteins by using an *Escherichia coli* strain unable to incorporate selenium from selenite into proteins, *Proc. Natl. Acad. Sci. U. S. A.* 99 (2002) 9150–9153.
- [37] L. Onate-Sanchez, J. Vicente-Carbajosa, DNA-free RNA isolation protocols for Arabidopsis thaliana, including seeds and siliques, *BMC Res. Notes* 1 (2008) 93.
- [38] T. Tzfira, G.W. Tian, B. Lacroix, S. Vyas, J. Li, Y. Leitner-Dagan, A. Krichevsky, T. Taylor, A. Vainstein, V. Citovsky, pSAT vectors: a modular series of plasmids for autofluorescent protein tagging and expression of multiple genes in plants, *Plant Mol. Biol.* 57 (2005) 503–516.
- [39] V. Citovsky, L.Y. Lee, S. Vyas, E. Glick, M.H. Chen, A. Vainstein, Y. Gafni, S.B. Gelvin, T. Tzfira, Subcellular localization of interacting proteins by bimolecular fluorescence complementation in planta, *J. Mol. Biol.* 362 (2006) 1120–1131.
- [40] L.Y. Lee, M.J. Fang, L.Y. Kuang, S.B. Gelvin, Vectors for multi-color bimolecular fluorescence complementation to investigate protein-protein interactions in living plant cells, *Plant Methods* 4 (2008) 24.
- [41] G. An, P.R. Ebert, A. Mitra, S.B. Ha, Binary vectors, in: S.B. Gelvin, R.A. Schilperoort, D.P.S. Verma (Eds.), *Plant Molecular Biology Manual*, Springer, Netherlands, Dordrecht, 1989, pp. 29–47.
- [42] A.M. Davis, A. Hall, A.J. Millar, C. Darrah, S.J. Davis, Protocol: streamlined sub-protocols for floral-dip transformation and selection of transformants in Arabidopsis thaliana, *Plant Methods* 5 (2009) 1–7.
- [43] F.-H. Wu, S.-C. Shen, L.-Y. Lee, S.-H. Lee, M.-T. Chan, C.-S. Lin, Tape-Arabidopsis sandwich—a simpler Arabidopsis protoplast isolation method, *Plant Methods* 5 (2009) 1–10.
- [44] A. Roy, A. Kucukural, Y. Zhang, I-TASSER: a unified platform for automated protein structure and function prediction, *Nat. Protoc.* 5 (2010) 725–738.
- [45] J. Yang, R. Yan, A. Roy, D. Xu, J. Poisson, Y. Zhang, The I-TASSER suite: protein structure and function prediction, *Nat. Methods* 12 (2015) 7–8.
- [46] C. The UniProt, UniProt: the universal protein knowledgebase, *Nucleic Acids Res.* 45 (2017) D158–D169.
- [47] J. Yang, A. Roy, Y. Zhang, Protein-ligand binding site recognition using complementary binding-specific substructure comparison and sequence profile alignment, *Bioinformatics (Oxf. Engl.)* 29 (2013) 2588–2595.
- [48] C. Dominguez, R. Boelens, A.M. Bonvin, HADDOCK: a protein-protein docking approach based on biochemical or biophysical information, *J. Am. Chem. Soc.* 125 (2003) 1731–1737.
- [49] G.C.P. van Zundert, J. Rodrigues, M. Trellet, C. Schmitz, P.L. Kastrius, E. Karaca, A.S.J. Melquiond, M. van Dijk, S.J. de Vries, A. Bonvin, The HADDOCK2.2 web server: user-friendly integrative modeling of biomolecular complexes, *J. Mol. Biol.* 428 (2016) 720–725.
- [50] L. Li, N. Cheng, K.D. Hirschi, X. Wang, Structure of Arabidopsis chloroplastic monothiol glutaredoxin AtGRXcp, *Acta Crystallogr. D Biol. Crystallogr.* 66 (2010) 725–732.

- [51] H.M. Berman, J. Westbrook, Z. Feng, G. Gilliland, T.N. Bhat, H. Weissig, I.N. Shindyalov, P.E. Bourne, The protein data bank, *Nucleic Acids Res.* 28 (2000) 235–242.
- [52] S.J. de Vries, A.M. Bonvin, CPOR: a consensus interface predictor and its performance in prediction-driven docking with HADDOCK, *PLoS One* 6 (2011) e17695.
- [53] E. Krissinel, K. Henrick, Inference of macromolecular assemblies from crystalline state, *J. Mol. Biol.* 372 (2007) 774–797.
- [54] Y. Balmer, B.B. Buchanan, Yet another plant thioredoxin, *Trends Plant Sci.* 7 (2002) 191–193.
- [55] S. Witte, M. Villalba, K. Bi, Y. Liu, N. Isakov, A. Altman, Inhibition of the c-Jun N-terminal kinase/AP-1 and NF- $\kappa$ B pathways by PICOT, a novel protein kinase C-interacting protein with a thioredoxin homology domain, *J. Biol. Chem.* 275 (2000) 1902–1909.
- [56] P. Haunhorst, C. Berndt, S. Eitner, J.R. Godoy, C.H. Lillig, Characterization of the human monothiol glutaredoxin 3 (PICOT) as iron-sulfur protein, *Biochem. Biophys. Res. Commun.* 394 (2010) 372–376.
- [57] U. Muhlenhoff, S. Molik, J.R. Godoy, M.A. Uzarska, N. Richter, A. Seubert, Y. Zhang, J. Stubbe, F. Pierrel, E. Herrero, C.H. Lillig, R. Lill, Cytosolic monothiol glutaredoxins function in intracellular iron sensing and trafficking via their bound iron-sulfur cluster, *Cell Metab.* 12 (2010) 373–385.
- [58] K. Anna, P. Ranjan Nath, M. Keren, I. Noah, PICOT: a multidomain protein with multiple functions, *ISRN Immunol.* 2011 (2011).
- [59] I.M. Nooren, J.M. Thornton, Diversity of protein-protein interactions, *EMBO J.* 22 (2003) 3486–3492.
- [60] N. Isakov, S. Witte, A. Altman, PICOT-HD: a highly conserved protein domain that is often associated with thioredoxin and glutaredoxin modules, *Trends Biochem. Sci.* 25 (2000) 537–539.
- [61] R. Raucci, G. Colonna, E. Guerriero, F. Capone, M. Accardo, G. Castello, S. Costantini, Structural and functional studies of the human selenium binding protein-1 and its involvement in hepatocellular carcinoma, *Biochim. Biophys. Acta* 1814 (2011) 513–522.
- [62] U.-H. Cho, N.-H. Seo, Oxidative stress in *Arabidopsis thaliana* exposed to cadmium is due to hydrogen peroxide accumulation, *Plant Sci.* 168 (2005) 113–120.
- [63] Y.S. Guo, C.J. Huang, Y. Xie, F.M. Song, X.P. Zhou, A tomato glutaredoxin gene SIGRX1 regulates plant responses to oxidative, drought and salt stresses, *Planta* 232 (2010) 1499–1509.
- [64] B. Touraine, J.P. Boutin, A. Marion-Poll, J.F. Briat, G. Peltier, S. Lobreaux, Nfu2: a scaffold protein required for [4Fe-4S] and ferredoxin iron-sulphur cluster assembly in *Arabidopsis* chloroplasts, *Plant J.* 40 (2004) 101–111.
- [65] P.W. Chang, S.K. Tsui, C. Liew, C.C. Lee, M.M. Wayne, K.P. Fung, Isolation, characterization, and chromosomal mapping of a novel cDNA clone encoding human selenium binding protein, *J. Cell. Biochem.* 64 (1997) 217–224.
- [66] G. Chen, H. Wang, C.T. Miller, D.G. Thomas, T.G. Gharib, D.E. Misek, T.J. Giordano, M.B. Orringer, S.M. Hanash, D.G. Beer, Reduced selenium-binding protein 1 expression is associated with poor outcome in lung adenocarcinomas, *J. Pathol.* 202 (2004) 321–329.
- [67] J.Y. Jeong, Y. Wang, A.J. Sytkowski, Human selenium binding protein-1 (hSP56) interacts with VDU1 in a selenium-dependent manner, *Biochem. Biophys. Res. Commun.* 379 (2009) 583–588.
- [68] S. Bandyopadhyay, F. Gama, M.M. Molina-Navarro, J.M. Gualberto, R. Claxton, S.G. Naik, B.H. Huynh, E. Herrero, J.P. Jacquot, M.K. Johnson, N. Rouhier, Chloroplast monothiol glutaredoxins as scaffold proteins for the assembly and delivery of [2Fe-2S] clusters, *EMBO J.* 27 (2008) 1122–1133.
- [69] X. Liu, S. Liu, Y. Feng, J.-Z. Liu, Y. Chen, K. Pham, H. Deng, K.D. Hirschi, X. Wang, N. Cheng, Structural insights into the N-terminal GIY-YIG endonuclease activity of *Arabidopsis* glutaredoxin AtGRXS16 in chloroplasts, *Proc. Natl. Acad. Sci. U. S. A.* 110 (2013) 9565–9570.
- [70] T.K. Kerppola, Bimolecular fluorescence complementation (BiFC) analysis as a probe of protein interactions in living cells, *Annu. Rev. Biophys.* 37 (2008) 465–487.
- [71] C. Fellerer, R. Schweiger, K. Schongrubler, J. Soll, S. Schwenkert, Cytosolic HSP90 cochaperones HOP and FKBP interact with freshly synthesized chloroplast pre-proteins of *Arabidopsis*, *Mol. Plant* 4 (2011) 1133–1145.
- [72] T. May, J. Soll, 14-3-3 proteins form a guidance complex with chloroplast precursor proteins in plants, *Plant Cell* 12 (2000) 53–64.
- [73] S. Qbadou, T. Becker, O. Mirus, I. Tews, J. Soll, E. Schleiff, The molecular chaperone Hsp90 delivers precursor proteins to the chloroplast import receptor Toc64, *EMBO J.* 25 (2006) 1836–1847.